

# Loop effects and non-decoupling property of SUSY QCD in $gb \rightarrow tH^-$

Guangping Gao <sup>a,b</sup>, Gongru Lu <sup>b</sup>, Zhaohua Xiong <sup>a,c</sup> and Jin Min Yang <sup>a</sup>

<sup>a</sup> *Institute of Theoretical Physics, Academia Sinica, Beijing 100080, China*

<sup>b</sup> *Physics Department, Henan Normal University, Xinxiang 453002, China*

<sup>c</sup> *Institute of High Energy Physics, Academia Sinica, Beijing 100039, China*

(February 8, 2020)

One-loop SUSY QCD radiative correction to  $gb \rightarrow tH^-$  cross section is calculated in the Minimal Supersymmetric Standard Model. We found that SUSY QCD is non-decoupling if the gluino mass and the parameter  $\mu$  or  $A_t$  or  $A_b$  are at the same order and get large. The non-decoupling contribution can be enhanced by large  $\tan\beta$  and therefore large corrections to the hadronic production rates at the Tevatron and LHC are expected in the large  $\tan\beta$  limit. The fundamental reason for such non-decoupling behavior is found to be some couplings in the loops being proportional to SUSY mass parameters.

14.80.Cp, 13.85.Qk,12.60.Jv

## I. INTRODUCTION

Although the Standard Model (SM) is phenomenologically successful, it is arguably an effective theory and new physics must exist at high energy scales. Among all elementary particles predicted by the SM, top quark and Higgs boson may hold the key to new physics since they are most related to the electroweak symmetry breaking. An intensive study of the properties of top quark and Higgs boson will be one of the primary tasks of particle physics in the new millennium.

So far the most intensively studied new physics model is the Minimal Supersymmetric Standard Model (MSSM) [1]. This model predicts the existence of five Higgs bosons,  $H^0$ ,  $h^0$ ,  $A^0$  and  $H^\pm$ , all of which couples to top quark. Compared to the couplings in the SM, the coupling  $tbH^-$  is an utterly new coupling. Previous studies [2] show that this coupling is subject to large quantum corrections and may be a good probe of the MSSM. Although this coupling could be measured from top quark decay process  $t \rightarrow H^+b$  for a light charged Higgs, the direct production of a top quark associated with a charged Higgs boson through the subprocess  $gb \rightarrow tH^-$  at hadron colliders will be a good probe for  $tbH^-$  coupling [3]. In this work we calculate the one-loop SUSY QCD corrections to this process owing to the following motivations. Firstly, this process at the Tevatron and LHC happens at a very high energy and has more loop diagrams and thus, is expected to be more sensitive to SUSY QCD corrections compared to some decay processes like  $t \rightarrow H^+b$  [4–6]. Secondly, some works [4–6] recently re-analyzed the one-loop SUSY QCD corrections to some decay processes like  $t \rightarrow H^+b$  and found SUSY QCD to be non-

decoupling in some cases. The process we will study may be an ideal place to investigate the property of SUSY QCD corrections. Moreover, as is well known, the decoupling theorem [7] states that under certain conditions in a given quantum field theory with light and heavy particles, if the heavy particles are integrated out to all orders in perturbation theory, the remaining effective action to be valid at energies much lower than the heavy particle masses does not show any trace of these heavy particles. If SUSY QCD is non-decoupling in some cases, we need a proper understanding.

This paper is organized as follows. In Section II we present the formula for the one-loop SUSY-QCD corrections to the  $gb \rightarrow tH^\pm$  process. In Section III we scan the parameter space of MSSM to estimate the size of SUSY-QCD corrections. In Section IV we study the decoupling behavior of SUSY QCD. A discussion on how the decoupling and non-decoupling take place is also given. Finally, the conclusions are summarized in Section V.

## II. CALCULATIONS

The subprocess  $gb \rightarrow tH^-$  occurs through both s-channel and t-channel. The tree-level amplitude is given by

$$M_0 = M_0^{(s)} + M_0^{(t)}, \quad (2.1)$$

where  $M_0^{(s)}$  and  $M_0^{(t)}$  represent the amplitudes arising from the s-channel diagram shown in Fig. 1(a) and the t-channel diagram shown in Fig. 1(b), respectively. They can be expressed as

$$M_0^{(s)} = \frac{igg_s V_{tb}}{\sqrt{2}m_W(\hat{s} - m_b^2)} \bar{u}(p_t) [2\eta_t p_b^\mu P_L + 2\eta_b p_b^\mu P_R - \eta_t \gamma^\mu \not{k} P_L - \eta_b \gamma^\mu \not{k} P_R] u(p_b) \varepsilon_\mu(k) T_{ij}^a, \quad (2.2)$$

$$M_0^{(t)} = \frac{igg_s V_{tb}}{\sqrt{2}m_W(\hat{t} - m_t^2)} \bar{u}(p_t) [2\eta_t p_t^\mu P_L + 2\eta_b p_t^\mu P_R - \eta_t \gamma^\mu \not{k} P_L - \eta_b \gamma^\mu \not{k} P_R] u(p_b) \varepsilon_\mu(k) T_{ij}^a, \quad (2.3)$$

where  $P_{R,L} \equiv (1 \pm \gamma_5)/2$ , and  $p_t$ ,  $p_b$  and  $k$  are the momenta of the outgoing top quark, the incoming bottom quark and the incoming gluon, respectively.  $\hat{s}$  and  $\hat{t}$  are the subprocess Mandelstam variables defined by  $\hat{s} = (p_b + k)^2 = (p_t + p_{H^-})^2$  and  $\hat{t} = (p_t - k)^2 = (p_{H^-} - p_b)^2$ .  $T^a$  are the  $SU(3)$  color matrices and  $\tan\beta = v_2/v_1$  is the ratio of the vacuum expectation values of the two Higgs

doublets. The constants  $\eta_{b,t}$  are defined by  $\eta_b = m_b \tan \beta$  and  $\eta_t = m_t \cot \beta$ .

The one-loop Feynman diagrams of SUSY QCD corrections are shown in Fig. 1(c)-(n). In our calculations we use dimensional regularization to control all the ultraviolet divergences in the virtual loop corrections and we adopt the on-mass-shell renormalization scheme. Including the one-loop SUSY QCD corrections, the renormalized amplitude for  $gb \rightarrow tH^-$  can be written as

$$M_{ren} = M_0^{(s)} + M_0^{(t)} + \delta M, \quad (2.4)$$

where  $\delta M$  represents the one-loop SUSY QCD corrections given by

$$\begin{aligned} \delta M = & \delta M^{V_1(s)} + \delta M^{V_2(s)} + \delta M^{s(s)} + \delta M^{box} \\ & + \delta M^{V_1(t)} + \delta M^{V_2(t)} + \delta M^{s(t)}. \end{aligned} \quad (2.5)$$

Here  $\delta M^{V_1(s)}$ ,  $\delta M^{V_2(s)}$  and  $\delta M^{s(s)}$  represent the renormalized vertex  $gb\bar{b}$ ,  $t\bar{b}H^-$  and the renormalized propagator in the s-channel diagram, respectively. Similar definitions are for  $\delta M^{V_1(t)}$ ,  $\delta M^{V_2(t)}$  and  $\delta M^{s(t)}$  in the t-channel diagram. The contribution of the box diagram is denoted by  $\delta M^{box}$ . Each  $\delta M^l$  can be decomposed as

$$\begin{aligned} \delta M^l = & \frac{igg_s^3 T_{ij}^a V_{tb}}{16\sqrt{2}\pi^2 m_W} C^l \bar{u}(p_t) \{ F_1^l \gamma^\mu P_L + F_2^l \gamma^\mu P_R \\ & + F_3^l p_b^\mu P_L + F_4^l p_b^\mu P_R + F_5^l p_t^\mu P_L + F_6^l p_t^\mu P_R \\ & + F_7^l \gamma^\mu \not{k} P_L + F_8^l \gamma^\mu \not{k} P_R + F_9^l p_b^\mu \not{k} P_L \\ & + F_{10}^l p_b^\mu \not{k} P_R + F_{11}^l p_t^\mu \not{k} P_L + F_{12}^l p_t^\mu \not{k} P_R \} \\ & u(p_b) \varepsilon_\mu(k), \end{aligned} \quad (2.6)$$

where the coefficients  $C^l$  and the form factors  $F_n^l$  are given explicitly in Appendix A and B, respectively. We have checked that all the ultraviolet divergences canceled as a result of renormalizability of MSSM.

The amplitude squared is given by

$$\begin{aligned} \overline{|M_{ren}|^2} = & \overline{|M_0^{(s)} + M_0^{(t)}|^2} \\ & + 2Re \overline{\sum} \left[ \left( M_0^{(s)} + M_0^{(t)} \right)^\dagger \delta M \right], \end{aligned} \quad (2.7)$$

where

$$\begin{aligned} \overline{|M_0^{(s)} + M_0^{(t)}|^2} = & \frac{2g^2 g_s^2 |V_{tb}|^2}{N_C m_W^2} \left\{ \frac{1}{(\hat{s} - m_b^2)^2} \right. \\ & \times [(\eta_b^2 + \eta_t^2)(p_b \cdot kp_t \cdot k + 2p_b \cdot kp_b \cdot \\ & - m_b^2 p_t \cdot kp_t - m_b^2 p_b \cdot p_t) + 2m_b^2 m_t^2 (p_b \cdot k - m_b^2)] \\ & + \frac{1}{(\hat{t} - m_t^2)^2} [(m_t^2 \cot^2 \beta + m_b^2 \tan^2 \beta)(p_b \cdot kp_t \cdot k \\ & + m_t^2 p_b \cdot k - m_t^2 p_b \cdot p_t) + 2m_b^2 m_t^2 (p_t \cdot k - m_t^2)] \\ & + \frac{1}{(\hat{s} - m_b^2)(\hat{t} - m_t^2)} [(\eta_b^2 + \eta_t^2)(2p_b \cdot kp_t \cdot k \\ & + 2p_b \cdot kp_b \cdot p_t - 2(p_b \cdot p_t)^2 - m_b^2 p_t \cdot k + m_t^2 p_b \cdot k) \\ & \left. + 2m_b^2 m_t^2 (p_t \cdot k - p_b \cdot k - 2p_b \cdot p_t)] \right\}, \end{aligned} \quad (2.8)$$

$$\begin{aligned} \overline{\sum} \left( M_0^{(s)} + M_0^{(t)} \right)^\dagger \delta M = & - \frac{g^2 g_s^4 |V_{tb}|^2}{64 N_C \pi^2 m_W^2} \\ & \times \sum_{n=1}^{12} \left[ \frac{1}{\hat{s} - m_b^2} h_n^{(s)} + \frac{1}{\hat{t} - m_t^2} h_n^{(t)} \right] C^l F_n^l. \end{aligned} \quad (2.9)$$

Here the color factor  $N_C = 3$ , and  $h_n^{(s)}$  and  $h_n^{(t)}$  can be found in Appendix A.

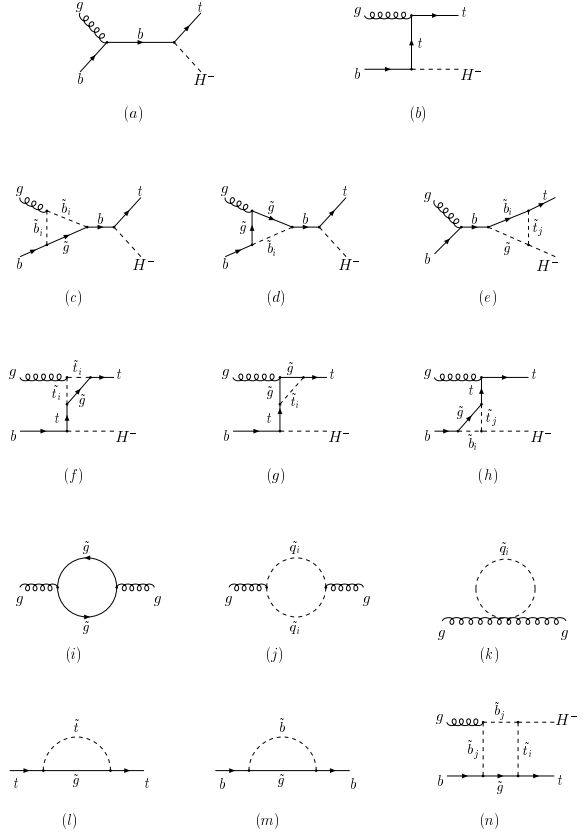


FIG. 1. Feynman diagrams of  $gb \rightarrow tH^-$  with one-loop SUSY QCD corrections: (a) and (b) are tree level diagrams; (c)–(e) are one-loop vertex diagrams for s-channel; (f)–(h) are one-loop vertex diagrams for t-channel; (i)–(m) are self-energy diagrams; (n) is the box diagram.

The cross section for the parton process  $gb \rightarrow tH^-$  is

$$\hat{\sigma}(\hat{s}) = \int_{\hat{t}_{min}}^{\hat{t}_{max}} \frac{1}{16\pi \hat{s}^2} \overline{\sum} |M_{ren}|^2 d\hat{t}, \quad (2.10)$$

with

$$\begin{aligned} \hat{t}_{max,min} = & \pm \sqrt{[\hat{s} - (m_t + m_{H^-})^2][\hat{s} - (m_t - m_{H^-})^2]} \\ & + \frac{m_t^2 + m_{H^-}^2 - \hat{s}}{4}. \end{aligned} \quad (2.11)$$

The total hadronic cross section for  $pp(\text{or } p\bar{p}) \rightarrow tH^- + X$  can be obtained by folding the subprocess cross section  $\hat{\sigma}$  with the parton luminosity

$$\sigma(s) = \int_{\tau_0}^1 d\tau \frac{dL}{d\tau} \hat{\sigma}(\hat{s} = s\tau), \quad (2.12)$$

where  $\tau_0 = (m_t + m_{H^-})^2/s$ , and  $s$  is the  $pp$ (or  $p\bar{p}$ ) center-of-mass energy squared.  $dL/d\tau$  is the parton luminosity given by

$$\frac{dL}{d\tau} = \int_{\tau}^1 \frac{dx}{x} [f_g^p(x, Q) f_b^p(\tau/x, Q) + (g \leftrightarrow b)], \quad (2.13)$$

where  $f_b^p$  and  $f_g^p$  are the bottom quark and gluon distribution functions in a proton, respectively. In our numerical calculation, we use the CTEQ5L parton distribution functions [8] with  $Q = m_t + m_{H^-}$ .

To show the size of the corrections, we define the relative quantity as

$$\Delta_{SQCD} = \frac{\sigma - \sigma_0}{\sigma_0}, \quad (2.14)$$

where  $\sigma_0$  is the tree-level cross section.

### III. NUMERICAL RESULTS

Before performing numerical calculations, we take a look at the relevant parameters involved.

For the SM parameters, we took  $m_W = 80.448$  GeV,  $m_Z = 91.187$  GeV,  $m_t = 176$  GeV,  $m_b = 4.5$  GeV. We used the two-loop running coupling constant  $\alpha_s(Q)$ .

For the SUSY parameters, apart from the charged Higgs mass, gluino mass and  $\tan\beta$ , the mass parameters of stops and sbottoms are involved. The mass square matrices of stop and sbottoms take the form ( $q = t$  or  $b$ ) [9]

$$M_q^2 = \begin{pmatrix} m_{\tilde{q}_L}^2 & m_q X_q^\dagger \\ m_q X_q & m_{\tilde{q}_R}^2 \end{pmatrix}, \quad (3.1)$$

where

$$\begin{aligned} m_{\tilde{q}_L}^2 &= m_{\tilde{Q}}^2 + m_q^2 - m_Z^2 \left( \frac{1}{2} + e_q \sin^2 \theta_W \right) \cos(2\beta), \\ m_{\tilde{q}_R}^2 &= m_{\tilde{U}, \tilde{D}}^2 + m_q^2 + e_q m_Z^2 \sin^2 \theta_W \cos(2\beta), \\ X_q &= \begin{cases} A_t - \mu \cot \beta, & \text{for } q = t, \\ A_b - \mu \tan \beta, & \text{for } q = b, \end{cases} \end{aligned} \quad (3.2)$$

Here  $m_{\tilde{Q}}^2$ ,  $m_{\tilde{U}}$  and  $m_{\tilde{D}}^2$  are soft-breaking mass terms for left-handed squark doublet  $\tilde{Q}$ , right-handed up squark  $\tilde{U}$  and down squark  $\tilde{D}$ , respectively.  $A_b(A_t)$  is the coefficient of the trilinear term  $H_1 \tilde{Q} \tilde{D}$  ( $H_2 \tilde{Q} \tilde{U}$ ) in soft-breaking terms and  $\mu$  the bilinear coupling of the two Higgs doublet in the superpotential. Thus the SUSY parameters involved in stop and sbottom mass matrices are

$$m_{\tilde{Q}}, m_{\tilde{U}}, m_{\tilde{D}}, A_t, A_b, \mu, \tan \beta.$$

The mass square matrices are diagonalized by unitary rotations ( $q = t$  or  $b$ )

$$R^q = \begin{pmatrix} \cos \theta_q & \sin \theta_q \\ -\sin \theta_q & \cos \theta_q \end{pmatrix} \quad (3.3)$$

which relates the weak-eigenstates ( $\tilde{q}_L, \tilde{q}_R$ ) to the mass eigenstates ( $\tilde{q}_1, \tilde{q}_2$ ). Then the stop and sbottom masses as well as the mixing angles are obtained by

$$\begin{aligned} m_{\tilde{t}_{1,2}} &= \frac{1}{2} \left[ m_{\tilde{q}_L}^2 + m_{\tilde{q}_R}^2 \pm \sqrt{(m_{\tilde{q}_L}^2 - m_{\tilde{q}_R}^2)^2 + 4X_q^2 X_t^2} \right], \\ \tan 2\theta_q &= \frac{2m_q X_q}{m_{\tilde{q}_L}^2 - m_{\tilde{q}_R}^2}. \end{aligned} \quad (3.4)$$

To determinate the mixing angles completely, we adopt the convention in [10] which sets  $\theta_q = \pi/4$  if  $m_{\tilde{q}_L} = m_{\tilde{q}_R}$  and shifts  $\pi/2$  to  $\theta_q$  if  $m_{\tilde{q}_L} > m_{\tilde{q}_R}$ . Thus  $\theta_q$  lies in the range  $-\frac{\pi}{4} \leq \theta_q \leq \frac{3}{4}\pi$ .

To find out the size of the one-loop SUSY QCD effects, we performed a scan over the nine-dimensional parameter space:  $m_{\tilde{Q}}, m_{\tilde{U}}, m_{\tilde{D}}, A_t, A_b, \mu, \tan\beta, m_{H^-}, m_{\tilde{g}}$ . In scanning we restricted  $m_{H^-}, A_t, A_b$  and  $\mu$  to the sub-TeV region and required  $m_{H^-} > 150$  GeV. Other mass parameters are assumed to be smaller than 5 TeV. In addition, we consider the following experimental constraints:

- (1)  $\mu > 0$  and a large  $\tan\beta$  in the range  $5 \leq \tan\beta \leq 50$ , which might be favored by the recent muon  $g - 2$  measurement [11].
- (2) The LEP and CDF lower mass bounds on gluino, stop and sbottom [12]

$$\begin{aligned} m_{\tilde{t}_1} &\geq 86.4 \text{ GeV}, m_{\tilde{b}_1} \geq 75.0 \text{ GeV}, \\ m_{\tilde{g}} &\geq 190 \text{ GeV}. \end{aligned} \quad (3.5)$$

The scan results are plotted in the plane of  $\Delta_{SQCD}$  versus  $\theta_b$  in Fig. 2.

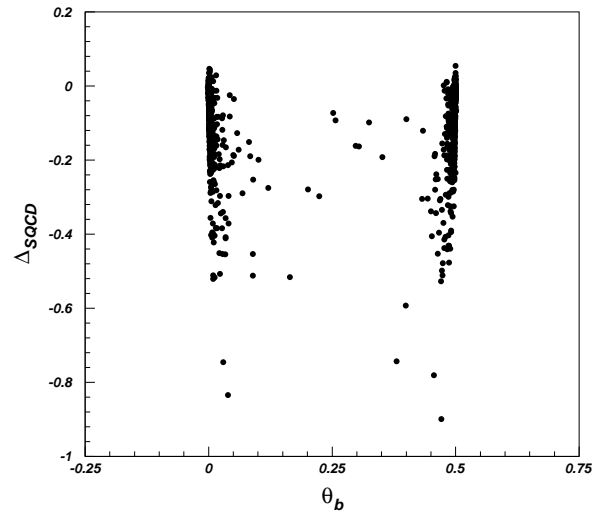


FIG. 2. The scatter plot in the plane of  $\Delta_{SQCD}$  versus  $\theta_b$ . The scan was performed over nine SUSY parameters.  $\theta_b$  is in unit of  $\pi$ .

From Fig. 2 one can see that in most parameter space the mixing of sbottoms is small while the one-loop SUSY QCD effect can be quite large. In some part of the parameter space, the correction size can be larger than 20% which cannot be neglected in the study of this process at LHC.

#### IV. DECOUPLING PROPERTY OF SUSY QCD

To find out if SUSY QCD is decoupling from the process  $gb \rightarrow tH^-$  in the large limit of SUSY mass parameters, we fix the charged Higgs mass as  $m_{H^-} = 250 \text{ GeV}$  and consider the following cases.

(1) *Scenario A*: All squark, gluino masses and  $\mu$  or  $A$  parameters are of the same size (collectively denoted by  $m_S$ ) and much heavier than the electroweak scale, i.e.,

$$\begin{aligned} m_S \sim m_{\tilde{Q}} \sim m_{\tilde{U}} \sim m_{\tilde{D}} \sim m_{\tilde{g}} \\ \sim \mu \text{ or } A_t \text{ or } A_b \sim m_S \gg M_{EW} \end{aligned} \quad (4.1)$$

In this case, both mixings in the sbottom and stop sectors reach their maximal values, i.e.,  $\theta_t \sim \pm \frac{\pi}{4}$ ,  $\theta_b \sim \pm \frac{\pi}{4}$ . As shown in Eqs. (5.3-5.5), the couplings  $\alpha_{ij}$  in the vertex  $H^- \tilde{t}_i \tilde{b}_j$  are proportional to the linear combination of  $\mu + A_b \tan \beta$  and  $\mu + A_t \cot \beta$ . Considering that the couplings  $\alpha_{ij}$  are proportional to  $m_S$  as  $\mu$  or  $A_{t,b}$  gets large as  $m_S$ , and the loop scalar integral functions  $C_0$  goes to  $-1/2m_S^2$  as  $m_S \gg \hat{s}$ , one can infer that the terms  $\alpha_{ij} A_{ij}^{2(L,R)} C_0 m_{\tilde{g}}$  in  $F_n^{V_2(s,t)}$  which arise from the vertex correction to  $H^- tb$  do not vanish but go to a non-zero constant, showing a clear indication of *non-decoupling* behavior.

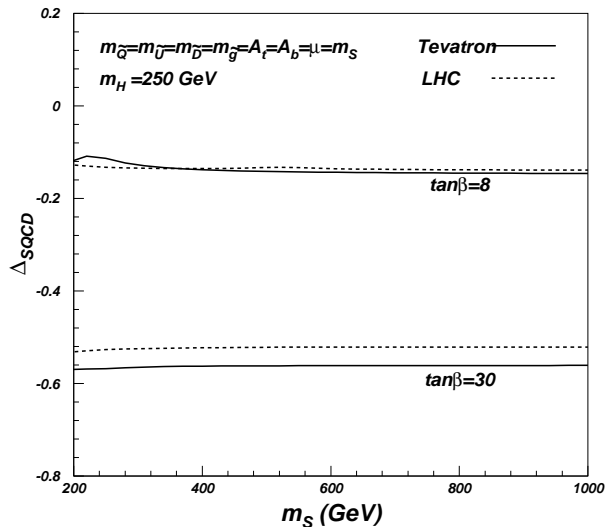


FIG. 3. Non-decoupling behavior of  $\Delta_{SQCD}$  with  $m_{\tilde{Q}} = m_{\tilde{U}} = m_{\tilde{D}} = m_{\tilde{g}} = A_b = A_t = \mu = m_S$  and for different values of  $\tan \beta$ . Corrections at the Tevatron with  $\sqrt{s} = 2 \text{ TeV}$  (solid lines) and at the LHC  $\sqrt{s} = 14 \text{ TeV}$  (dashed lines) are plotted respectively.

As illustrative examples, we plot the dependence of the one loop SUSY-QCD correction to  $gb \rightarrow tH^-$  on the common SUSY parameter  $m_S$  in Fig. 3. From this figure one can see the non-decoupling effects clearly. As for the dependence of the non-decoupling on  $\tan \beta$ , it is quite involved and complicated. For the parameter values chosen in our numerical examples, the corrections are enhanced by  $\tan \beta$ .

(2) *Scenario B*: The gluino mass and  $\mu$  are of the same order (collectively denoted by  $m_S$ ) and get much larger than squark masses and electroweak scale, i.e.,

$$m_S \sim m_{\tilde{g}} \sim \mu \gg m_{\tilde{Q}} \sim m_{\tilde{U}} \sim m_{\tilde{D}} \geq M_{EW} \quad (4.2)$$

To keep stop and sbottom masses from getting large, we can set  $A_t \simeq \mu \cot \beta$ ,  $A_b \simeq \mu \tan \beta$ . In this scenario, no mixings occur in the sbottom and stop sectors. Note that in this case, apart from the vertex correction discussed in Scenario A, the terms  $\alpha_{ij} A_{ij}^{2(L,R)} D_0 m_{\tilde{g}}$  in the box contribution (see Eq. (5.14)) do not vanish either since the four-point integral functions  $D_0 \rightarrow 1/m_S^2$  when  $m_S \gg \hat{s}$ . So in this case the SUSY QCD is non-decoupling. Although the non-decoupling effects can arise from more diagrams in this case, the reason is the same as in Scenario A, i.e., the couplings  $H^- \tilde{t}_i \tilde{b}_j$  are proportional to  $\mu$ .

(3) *Scenario C*: Only the gluino mass is very large than other SUSY parameters and the electroweak scale

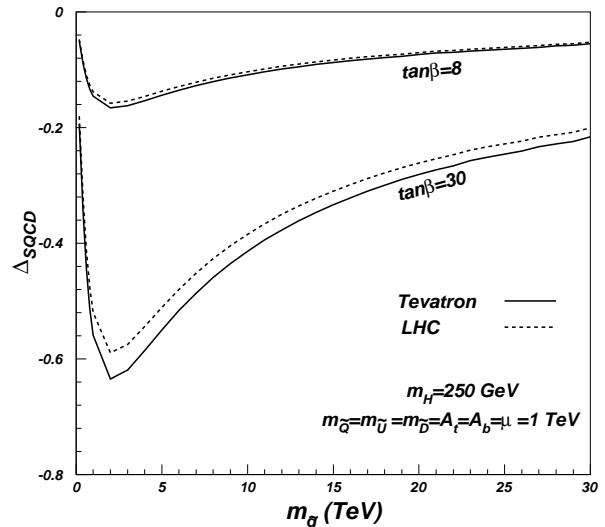


FIG. 4. Behavior of  $\Delta_{SQCD}$  in the large  $m_{\tilde{g}}$  limit with fixed  $m_{\tilde{Q}} = m_{\tilde{U}} = m_{\tilde{D}} = A_b = A_t = \mu = 1 \text{ TeV}$  and for different values of  $\tan \beta$ . The solid and dashed lines correspond to corrections at the Tevatron with  $\sqrt{s} = 2 \text{ TeV}$  and at the LHC  $\sqrt{s} = 14 \text{ TeV}$ , respectively.

In this scenario, to simplify the calculation we assumed  $m_{\tilde{Q}} = m_{\tilde{U}} = m_{\tilde{D}} = \mu = A_t = A_b = 1 \text{ TeV}$ . As shown in Fig. 4, the SUSY-QCD decouples. The reason is the scalar function like  $C_0$  goes like  $\sim -1/2m_{\tilde{g}}^2$  when  $m_{\tilde{g}}^2 \gg$

$\hat{s}$  but the couplings  $\alpha_{ij}$  in the vertex  $H^- \tilde{t}_i \tilde{b}_j$  are fixed, and thus the SUSY QCD correction goes like  $\sim 1/m_{\tilde{g}}$ . However, due to large collider beam energies and  $\hat{s}$  can be up to  $s$ , the decoupling is very slow, especially, at LHC, as shown in the figure.

From Fig. 3 and 4, one sees that the size of  $\Delta_{SQCD}$  can be quite large for large  $\tan\beta$ . Note that when one-loop effects are too large, higher-level loops must be also calculated. We refer the reader to [13] where some techniques of resummation for a better convergence are proposed.

(4) *Scenario D*: Only squark masses are of the same order (collectively denoted by  $m_S$ ) and very large than other SUSY parameters and the electroweak scale

As shown in Fig. 5, the SUSY QCD also decouples. In this case, it decouples much faster than in Scenario C where only gluino mass gets large. This can be understood easily because in this case the couplings  $\alpha_{ij}$  in the vertex  $H^- \tilde{t}_i \tilde{b}_j$  and the mass of gluino are both fixed, so that the terms like  $\alpha_{ij} A_{ij}^{2L} C_0 m_{\tilde{g}}$  go like  $\sim 1/m_S^2$ , where the square inverse suppression comes from the scalar function  $C_0$ .

From the above analysis we find that the fundamental reason for such non-decoupling behavior of SUSY QCD in the process  $gb \rightarrow tH^\pm$  is that some couplings like  $H^- \tilde{t}_i \tilde{b}_j$  are proportional to SUSY mass parameters. This is similar to the non-decoupling property of the heavy top quark in the SM, where the top quark Yukawa couplings are proportional to top quark mass.

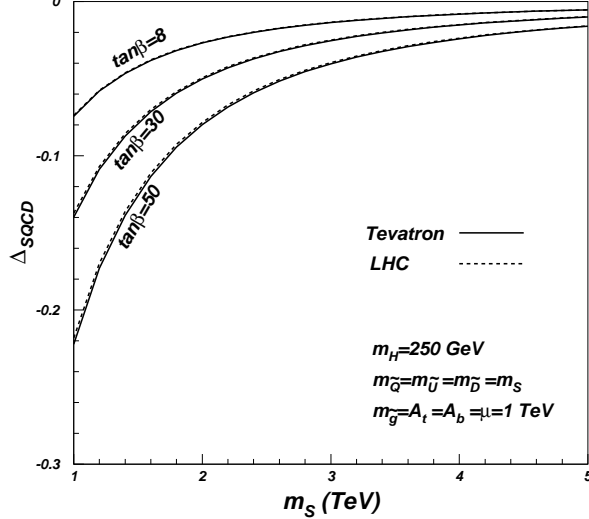


FIG. 5. Behavior of  $\Delta_{SQCD}$  in the large squark masses limit with fixed  $m_{\tilde{g}} = A_b = A_t = \mu = 1$  TeV and for different values of  $\tan\beta$ . The solid and dashed lines correspond to corrections at the Tevatron with  $\sqrt{s} = 2$  TeV and at the LHC  $\sqrt{s} = 14$  TeV, respectively.

As pointed out in the introduction, some works [4–6] recently also found similar non-decoupling behaviors of SUSY QCD in some decay process like  $t \rightarrow H^+ b$ . Al-

though the processes are different, the fundamental reason for such non-decoupling behavior pointed out in this work applies to their cases.

## V. CONCLUSIONS

In this work we have evaluated SUSY QCD radiative corrections to the  $gb \rightarrow tH^\pm$  at Tevatron and LHC. We have found that in some parameter space the one-loop SUSY-QCD correction can be quite large and cannot be neglected. We have discussed in detail on the decoupling behavior of the corrections in the large SUSY mass limit, and found that with fixed gluino mass the one-loop SUSY QCD corrections decouple; while non-decoupling occurs when gluino mass and  $\mu$  or  $A$  parameters both get large. We pointed out that such non-decoupling behavior arises from the  $H^- \tilde{t}_i \tilde{b}_j$  vertices which are proportional to SUSY mass parameters. Such large non-decoupling effects may play an important role in the indirect search for SUSY from the production of a top quark associated with a charged Higgs boson at Tevatron and LHC.

## ACKNOWLEDGMENT

This work is supported in part by a grant of Chinese Academy of Science for Outstanding Young Scholars.

## APPENDIX A

In this appendix we list the coefficients  $C^l$ , scalar functions  $h_n^{(l)}$  and the vertex  $V(H^- \tilde{t}_i \tilde{b}_j) = ig\alpha_{ij}/\sqrt{2}m_W$  ( $i, j = 1, 2$ ) needed in our calculations.

- Coefficients  $C^l$

$$\begin{aligned} C^{V(s)} &= \frac{1}{\hat{s} - m_b^2}, C^{V(t)} = \frac{1}{\hat{t} - m_t^2}, \\ C^{s(s)} &= \frac{1}{(\hat{s} - m_b^2)^2}, C^{s(t)} = \frac{1}{(\hat{t} - m_t^2)^2}, \\ C^{box} &= 1. \end{aligned} \quad (5.1)$$

- Scalar functions  $h_n^{(l)}$

$$\begin{aligned} h_1^{(l)} &= 4m_t\eta_t(2p_b \cdot k - p^{(l)} \cdot p_b) - 4m_b\eta_b(p^{(l)} \cdot p_t + p_t \cdot k), \\ h_2^{(l)} &= h_1^{(l)}(\eta_b \leftrightarrow \eta_t), \\ h_3^{(l)} &= 2\eta_t(2p_b \cdot kp_b \cdot p_t - m_b^2 p_t \cdot k - 2p^{(l)} \cdot p_b p_b \cdot p_t) \\ &\quad + 2m_b m_t \eta_b (p_b \cdot k - 2p^{(l)} \cdot p_b), \\ h_4^{(l)} &= h_3^{(l)}(\eta_b \leftrightarrow \eta_t), \\ h_5^{(l)} &= 2\eta_t(m_t^2 p_b \cdot k - 2p^{(l)} \cdot p_t p_b \cdot p_t) \\ &\quad + 2m_b m_t \eta_b (p_t \cdot k - 2p^{(l)} \cdot p_t), \end{aligned}$$

$$\begin{aligned}
h_6^{(l)} &= h_5^{(l)}(\eta_b \leftrightarrow \eta_t), \\
h_7^{(l)} &= 4\eta_t(p^{(l)} \cdot p_b p_t \cdot k - p^{(l)} \cdot k p_b \cdot p_t - p_b \cdot k p^{(l)} \cdot p_t \\
&\quad - 2p_b \cdot k p_t \cdot k) - 4m_b m_t \eta_b p^{(l)} \cdot k, \\
h_8^{(l)} &= h_7^{(l)}(\eta_b \leftrightarrow \eta_t), \\
h_9^{(l)} &= 4m_t \eta_t p_b \cdot k(p_b \cdot k - p^{(l)} \cdot p_b) - 4m_b \eta_b p^{(l)} \cdot p_b p_t \cdot k, \\
h_{10}^{(l)} &= h_9^{(l)}(\eta_b \leftrightarrow \eta_t), \\
h_{11}^{(l)} &= 4m_t \eta_t p_b \cdot k(p_t \cdot k - p^{(l)} \cdot p_t) - 4m_b \eta_b p_t \cdot k p^{(l)} \cdot p_t, \\
h_{12}^{(l)} &= h_{11}^{(l)}(\eta_b \leftrightarrow \eta_t), \tag{5.2}
\end{aligned}$$

where the index  $l$  represents the two channels  $s$  and  $t$ , and  $p^{(s)} = p_b$ ,  $p^{(t)} = p_t$ .

- Couplings of  $H^- \tilde{t}_i \tilde{b}_j$

The  $H^- \tilde{t}_i \tilde{b}_j$  interaction terms can be parametrized as

$$\mathcal{L}_{H^- \tilde{t}_i \tilde{b}_j} = \frac{g}{\sqrt{2}m_W} \alpha_{ij} \quad (i, j = 1, 2), \tag{5.3}$$

where

$$\begin{aligned}
\alpha_{ij} &= R_{i1}^{t*} R_{j1}^b g_{LL} + R_{i2}^{t*} R_{j2}^b g_{RR} \\
&\quad + R_{i1}^{t*} R_{j2}^b g_{LR} + R_{i2}^{t*} R_{j1}^b g_{RL}, \tag{5.4}
\end{aligned}$$

with

$$\begin{aligned}
g_{LL} &= -m_W^2 \sin 2\beta + m_b^2 \tan \beta + m_t^2 \cot \beta, \\
g_{RR} &= m_b m_t (\tan \beta + \cot \beta), \\
g_{LR} &= m_b (\mu + A_b \tan \beta), \\
g_{RL} &= m_t (\mu + A_t \cot \beta). \tag{5.5}
\end{aligned}$$

## APPENDIX B

The form factors  $F_n^l$  raise from the renormalized vertices and propagators of s-channel and t-channel, as well as box diagram given as following.

- The renormalized vertices of s-channel:

$$\begin{aligned}
F_1^{V_1(s)} &= \frac{4}{3} A_{bi}^2 \eta_b m_b C_{24} (-p_b, -k, m_{\bar{g}}, m_{\bar{b}_i}, m_{\bar{b}_i}) \\
&\quad - 3\eta_b \{ m_b p_b \cdot k (C_0 + C_{11}) + A_{bi}^1 m_{\bar{g}} p_b \cdot k C_0 \\
&\quad + A_{bi}^2 m_b [\hat{s} C_0 + m_b^2 (C_0 + 4C_{11} + 2C_{21}) \\
&\quad + 2p_b \cdot k (C_{11} + 2C_{12} + 2C_{23}) - 2m_{\bar{g}}^2 C_0 - 1 \\
&\quad + 4C_{24}] \} (p_b, k, m_{\bar{b}_i}, m_{\bar{g}}, m_{\bar{g}}) \\
&\quad + \frac{16\pi^2}{g_s^2} \eta_t m_b (\delta Z_L^b - \delta Z_R^b), \\
F_2^{V_1(s)} &= F_1^{V_1(s)} (\eta_b \rightarrow \eta_t, A_{bi}^2 \rightarrow -A_{bi}^2, R \leftrightarrow L), \\
F_3^{V_1(s)} &= \frac{2}{3} \eta_t \{ - [m_b^2 (C_{11} + C_{21}) + p_b \cdot k (C_{12} + C_{23})
\end{aligned}$$

$$\begin{aligned}
&\quad + C_{24}] + A_{bi}^1 m_{\bar{g}} m_b (C_0 + C_{11}) + 2A_{bi}^2 [C_{24} \\
&\quad + p_b \cdot k (C_{12} + C_{23})] \} (-p_b, -k, m_{\bar{g}}, m_{\bar{b}_i}, m_{\bar{b}_i}) \\
&\quad - 3\eta_t \{ [m_b^2 (C_0 + 2C_{11} + C_{21}) + m_{\bar{g}}^2 C_0 \\
&\quad - 2C_{24} + 1/2] + 2A_{bi}^1 m_b m_{\bar{g}} (C_0 + C_{11}) \\
&\quad + 2A_{bi}^2 [m_b^2 (C_0 + 2C_{11} + C_{21}) - m_{\bar{g}}^2 C_0 \\
&\quad - 1/2 + 2C_{24}] \} (p_b, k, m_{\bar{b}_i}, m_{\bar{g}}, m_{\bar{g}}) \\
&\quad - \frac{16\pi^2}{g_s^2} \eta_t 2\delta Z_R^b,
\end{aligned}$$

$$F_4^{V_1(s)} = F_3^{V_1(s)a} (\eta_t \rightarrow \eta_b, A_{bi}^2 \rightarrow -A_{bi}^2, R \leftrightarrow L),$$

$$\begin{aligned}
F_7^{V_1(s)} &= \frac{1}{3} \eta_t (C_{24} - 2A_{bi}^2 C_{24}) (-p_b, -k, m_{\bar{g}}, m_{\bar{b}_i}, m_{\bar{b}_i}) \\
&\quad - \frac{3}{2} \eta_t \{ m_b^2 (C_{21} - C_0) + 2p_b \cdot k (C_{12} + C_{23}) \\
&\quad - m_{\bar{g}}^2 C_0 + 2C_{24} - 1/2) - 2A_{bi}^1 m_b m_{\bar{g}} C_0 \\
&\quad - 2A_{bi}^2 [m_b^2 (C_0 + 2C_{11} + C_{21}) + 2p_b \cdot k (C_{12} + C_{23}) \\
&\quad - m_{\bar{g}}^2 C_0 - 1/2 + 2C_{24}] \} (p_b, k, m_{\bar{b}_i}, m_{\bar{g}}, m_{\bar{g}}) \\
&\quad + \frac{16\pi^2}{g_s^2} \eta_t \delta Z_R^b,
\end{aligned}$$

$$F_8^{V_1(s)} = F_7^{V_1(s)} (\eta_t \rightarrow \eta_b, A_{bi}^2 \rightarrow -A_{bi}^2, R \leftrightarrow L),$$

$$F_9^{V_1(s)} = \frac{1}{3} \eta_b [-m_b (C_{11} + C_{21}) + A_{bi}^1 m_{\bar{g}} (C_0 + C_{11})$$

$$\begin{aligned}
&\quad + 2A_{bi}^2 m_b (2C_{12} + 2C_{23} - C_{11} \\
&\quad - C_{21})] (-p_b, -k, m_{\bar{g}}, m_{\bar{b}_i}, m_{\bar{b}_i}) \\
&\quad - 3\eta_b [m_b (C_{11} + C_{21}) + A_{bi}^1 m_{\bar{g}} C_{11} + 2A_{bi}^2 m_b (C_{11} \\
&\quad + C_{21} - 2C_{12} - 2C_{23})] (p_b, k, m_{\bar{b}_i}, m_{\bar{g}}, m_{\bar{g}}),
\end{aligned}$$

$$F_{10}^{V_1(s)} = F_9^{V_1(s)} (\eta_b \rightarrow \eta_t, A_{bi}^2 \rightarrow -A_{bi}^2), \tag{5.6}$$

$$F_1^{V_2(s)} = \frac{8}{3} \alpha_{ij} A_{ij}^{1R} p_b \cdot k C_{12} (-p_t, -p_{H^-}, m_{\bar{g}}, m_{\bar{t}_i}, m_{\bar{b}_j}),$$

$$F_2^{V_2(s)} = F_1^{V_2(s)} (R \leftrightarrow L),$$

$$\begin{aligned}
F_3^{V_2(s)} &= \frac{8}{3} \alpha_{ij} [A_{ij}^{1R} m_t (C_{11} - C_{12}) + A_{ij}^{1L} m_b C_{12} \\
&\quad - m_{\bar{g}} A_{ij}^{2L} C_0] (-p_t, -p_{H^-}, m_{\bar{g}}, m_{\bar{t}_i}, m_{\bar{b}_j}),
\end{aligned}$$

$$F_4^{V_2(s)} = F_3^{V_2(s)} (R \leftrightarrow L),$$

$$\begin{aligned}
F_7^{V_2(s)} &= -\frac{4}{3} \alpha_{ij} [A_{ij}^{1R} m_t (C_{11} - C_{12}) + A_{ij}^{1L} m_b C_{12} \\
&\quad - A_{ij}^{2L} m_{\bar{g}} C_0] (-p_t, -p_{H^-}, m_{\bar{g}}, m_{\bar{t}_i}, m_{\bar{b}_j}),
\end{aligned}$$

$$F_8^{V_2(s)} = F_7^{V_2(s)} (R \leftrightarrow L). \tag{5.7}$$

- The renormalized vertices of t-channel:

$$\begin{aligned}
F_1^{V_1(t)} &= \frac{4}{3} A_{ti}^2 \eta_t m_t C_{24} (-p_t, k, m_{\bar{g}}, m_{\bar{t}_i}, m_{\bar{t}_i}) \\
&\quad + 3\eta_t \{ A_{ti}^1 m_t p_t \cdot k (C_0 + C_{11}) + A_{ti}^1 m_{\bar{g}} p_t \cdot k C_0 \\
&\quad - A_{ti}^2 m_t [\hat{t} C_0 + m_t^2 (C_0 + 4C_{11} + 2C_{21}) \\
&\quad - 2p_t \cdot k (C_{11} + 2C_{12} + 2C_{23}) - 2m_{\bar{g}}^2 C_0
\end{aligned}$$

$$\begin{aligned}
& -1 + 4C_{24}]] \} (-p_t, k, m_{\bar{t}_i}, m_{\bar{g}}, m_{\bar{g}}) \\
& - \frac{16\pi^2}{g_s^2} \eta_t m_t (\delta Z_R^t - \delta Z_L^t), \\
F_2^{V_1(t)} &= F_1^{V_1(t)a} (\eta_t \rightarrow \eta_b, A_{\bar{t}_i}^2 \rightarrow -A_{\bar{t}_i}^2, R \leftrightarrow L), \\
F_5^{V_1(t)} &= \frac{2}{3} \eta_t \{ - [m_t^2 (C_{11} + C_{21}) - p_t \cdot k (C_{12} + C_{23}) \\
& + C_{24}] + A_{\bar{t}_i}^1 m_{\bar{g}} m_t (C_0 + C_{11}) + 2A_{\bar{t}_i}^2 [-C_{24} \\
& + p_t \cdot k (C_{12} + C_{23})] \} (-p_t, k, m_{\bar{g}}, m_{\bar{t}_i}, m_{\bar{t}_i}) \\
& - 3\eta_t \{ [m_t^2 (C_0 + 2C_{11} + C_{21}) + m_{\bar{g}}^2 C_0 \\
& - 2C_{24} + 1/2] + 2A_{\bar{t}_i}^1 m_t m_{\bar{g}} (C_0 + C_{11}) \\
& - 2A_{\bar{t}_i}^2 [m_t^2 (C_0 + 2C_{11} + C_{21}) - m_{\bar{g}}^2 C_0 \\
& - 1/2 + 2C_{24}] \} (-p_t, k, m_{\bar{t}_i}, m_{\bar{g}}, m_{\bar{g}}) \\
& - \frac{16\pi^2}{g_s^2} \eta_t 2\delta Z_R^t, \\
F_6^{V_1(t)} &= F_5^{V_1(t)} (\eta_t \rightarrow \eta_b, A_{\bar{t}_i}^2 \rightarrow -A_{\bar{t}_i}^2, R \leftrightarrow L), \\
F_7^{V_1(t)} &= \frac{1}{3} \eta_t (C_{24} + 2A_{\bar{t}_i}^2 C_{24}) (-p_t, k, m_{\bar{g}}, m_{\bar{t}_i}, m_{\bar{t}_i}) \\
& + \frac{3}{2} \eta_t \{ Bi^1 [m_t^2 (C_0 - C_{21}) + 2p_t \cdot k (C_{12} + C_{23}) \\
& + m_{\bar{g}}^2 C_0 - 2C_{24} + 1/2] + 2A_{\bar{t}_i}^1 m_t m_{\bar{g}} C_0 \\
& - 2A_{\bar{t}_i}^2 [m_t^2 (C_0 + 2C_{11} + C_{21}) - 2p_t \cdot k (C_{12} + C_{23}) \\
& - m_{\bar{g}}^2 C_0 - 1/2 + 2C_{24}] \} (-p_t, k, m_{\bar{t}_i}, m_{\bar{g}}, m_{\bar{g}}) \\
& + \frac{16\pi^2}{g_s^2} \eta_t \delta Z_R^t, \\
F_8^{V_1(t)} &= F_7^{V_1(t)} (\eta_t \rightarrow \eta_b, A_{\bar{t}_i}^2 \rightarrow -A_{\bar{t}_i}^2, R \leftrightarrow L), \\
F_{11}^{V_1(t)} &= \frac{1}{3} \eta_t [m_t (C_{11} + C_{21}) - A_{\bar{t}_i}^1 m_{\bar{g}} (C_0 + C_{11}) \\
& - 2A_{\bar{t}_i}^2 m_t (2C_{12} + 2C_{23} - C_{11} \\
& - C_{21})] (-p_t, k, m_{\bar{g}}, m_{\bar{t}_i}, m_{\bar{t}_i}) \\
& + 3\eta_t [m_t (C_{11} + C_{21}) + A_{\bar{t}_i}^1 m_{\bar{g}} C_{11} + A_{\bar{t}_i}^2 2m_t (C_{11} \\
& + C_{21} - 2C_{12} - 2C_{23})] (-p_t, k, m_{\bar{t}_i}, m_{\bar{g}}, m_{\bar{g}}), \\
F_{12}^{V_1(t)} &= F_{11}^{V_1(t)} (\eta_t \rightarrow \eta_b, A_{\bar{t}_i}^2 \rightarrow -A_{\bar{t}_i}^2), \quad (5.8) \\
F_1^{V_2(t)} &= -\frac{8}{3} \alpha_{ij} A_{ij}^{1R} p_t \cdot k C_{12} (-p_b, p_{H^-}, m_{\bar{g}}, m_{\bar{b}_j}, m_{\bar{t}_i}), \\
F_2^{V_2(t)} &= F_1^{V_2(t)} (R \leftrightarrow L), \\
F_5^{V_2(t)} &= \frac{8}{3} \alpha_{ij} [A_{ij}^{1L} m_b (C_{11} - C_{12}) A_{ij}^{1R} m_t C_{12} \\
& - A_{ij}^{2L} m_{\bar{g}} C_0] (-p_b, p_{H^-}, m_{\bar{g}}, m_{\bar{b}_j}, m_{\bar{t}_i}), \\
F_6^{V_2(t)} &= F_5^{V_2(t)} (R \leftrightarrow L), \\
F_7^{V_2(t)} &= -\frac{4}{3} \alpha_{ij} [A_{ij}^{1L} m_b (C_{11} - C_{12}) + A_{ij}^{1R} m_t C_{12} \\
& - A_{ij}^{2L} m_{\bar{g}} C_0] (-p_b, p_{H^-}, m_{\bar{g}}, m_{\bar{b}_j}, m_{\bar{t}_i}), \\
F_8^{V_2(t)} &= F_7^{V_2(t)} (R \leftrightarrow L).
\end{aligned}$$

- The renormalized propagator of s-channel:

$$\begin{aligned}
F_1^{s(s)} &= \frac{16\pi^2}{g_s^2} \eta_b [2m_b p_b \cdot k (\hat{\Sigma}_L^b + \hat{\Sigma}_S^b)], \\
F_2^{s(s)} &= F_1^{s(s)} (\eta_b \rightarrow \eta_t, R \leftrightarrow L), \\
F_3^{s(s)} &= \frac{16\pi^2}{g_s^2} \eta_t [2 (\hat{s} \hat{\Sigma}_L^b + m_b^2 \hat{\Sigma}_R^b) + 4m_b^2 \hat{\Sigma}_S^b], \\
F_4^{s(s)} &= F_3^{s(s)} (\eta_t \rightarrow \eta_b, R \leftrightarrow L), \\
F_7^{s(s)} &= -\frac{16\pi^2}{g_s^2} \eta_t [\hat{s} \hat{\Sigma}_L^b + m_b^2 \hat{\Sigma}_R^b + 2m_b^2 \hat{\Sigma}_S^b], \\
F_8^{s(s)} &= F_7^{s(s)} (\eta_t \rightarrow \eta_b, R \leftrightarrow L). \quad (5.10)
\end{aligned}$$

- The renormalized propagator of t-channel:

$$\begin{aligned}
F_1^{s(t)} &= -\frac{16\pi^2}{g_s^2} \eta_t [2m_t p_t \cdot k (\hat{\Sigma}_L^t + \hat{\Sigma}_S^t)], \\
F_2^{s(t)} &= F_1^{s(t)} (\eta_t \rightarrow \eta_b, R \leftrightarrow L), \\
F_5^{s(t)} &= \frac{16\pi^2}{g_s^2} \eta_t [2 (\hat{t} \hat{\Sigma}_R^t + m_t^2 \hat{\Sigma}_L^t) + 4m_t^2 \hat{\Sigma}_S^t], \\
F_6^{s(t)} &= F_5^{s(t)} (\eta_t \rightarrow \eta_b, R \leftrightarrow L), \\
F_7^{s(t)} &= -\frac{16\pi^2}{g_s^2} \eta_t [\hat{t} \hat{\Sigma}_R^t + m_t^2 \hat{\Sigma}_L^t + 2m_t^2 \hat{\Sigma}_S^t], \\
F_8^{s(t)} &= F_7^{s(t)} (\eta_t \rightarrow \eta_b, R \leftrightarrow L). \quad (5.11)
\end{aligned}$$

- Box diagram contribution:

$$\begin{aligned}
F_1^{box} &= -\frac{1}{3} \alpha_{ij} A_{ij}^{1R} D_{27} (-p_b, -k, p_{H^-}, m_{\bar{g}}, m_{\bar{b}_j}, m_{\bar{b}_j}, m_{\bar{t}_i}), \\
F_2^{box} &= F_1^{box} (R \leftrightarrow L), \\
F_3^{box} &= \frac{1}{3} \alpha_{ij} [m_b A_{ij}^{1L} (D_{13} - D_{11} - D_{21} - D_{23} + 2D_{25}) \\
& - m_t A_{ij}^{1R} (D_{13} + D_{25} - D_{23}) + m_{\bar{g}} A_{ij}^{2L} (D_0 + D_{11} \\
& - D_{13})] (-p_b, -k, p_{H^-}, m_{\bar{g}}, m_{\bar{b}_j}, m_{\bar{b}_j}, m_{\bar{t}_i}), \\
F_4^{box} &= F_3^{box} (R \leftrightarrow L), \\
F_5^{box} &= \frac{1}{3} \alpha_{ij} [A_{ij}^{1L} (D_{23} - D_{25}) m_b - m_t A_{ij}^{1R} D_{23} \\
& + A_{ij}^{2L} m_{\bar{g}} D_{13}] (-p_b, -k, p_{H^-}, m_{\bar{g}}, m_{\bar{b}_j}, m_{\bar{b}_j}, m_{\bar{t}_i}), \\
F_6^{box} &= F_5^{box} (R \leftrightarrow L), \\
F_9^{box} &= \frac{1}{3} \alpha_{ij} A_{ij}^{1R} (D_{13} - D_{12} - D_{24} - D_{23} + D_{25} \\
& + D_{26}) (-p_b, -k, p_{H^-}, m_{\bar{g}}, m_{\bar{b}_j}, m_{\bar{b}_j}, m_{\bar{t}_i}), \\
F_{10}^{box} &= F_9^{box} (R \leftrightarrow L), \\
F_{11}^{box} &= \frac{1}{3} \alpha_{ij} A_{ij}^{1R} (D_{23} \\
& - D_{26}) (-p_b, -k, p_{H^-}, m_{\bar{g}}, m_{\bar{b}_j}, m_{\bar{b}_j}, m_{\bar{t}_i}), \\
F_{12}^{box} &= F_{11}^{box} (R \leftrightarrow L). \quad (5.9)
\end{aligned} \quad (5.12)$$

Here  $A_{(t,b)i}^1 = (-1)^i \sin 2\theta_{t,b}$ ,  $A_{(t,b)i}^2 = \frac{1}{2} (-1)^i \cos 2\theta_{t,b}$ .  $A_{ij}$  are defined as  $A_{ij}^{1L} = 2R_{i2}^t R_{j2}^b$ ,  $A_{ij}^{1R} = 2R_{i1}^t R_{j1}^b$ ,

$A_{ij}^{2L} = -2R_{i2}^t R_{j1}^b$  and  $A_{ij}^{2R} = -2R_{i1}^t R_{j2}^b$ . All other form factors  $F_n^l$  not listed above vanish. Note in the above formula we take the convention that repeated indices are summed over.

The renormalization constants appearing in the above form factors are given by

$$\begin{aligned}
\delta Z_L^t &= -\frac{g_s^2 C_F}{16\pi^2} \left\{ m_t \left[ 2m_t \frac{\partial B_1}{\partial p_t^2} - m_{\bar{g}} A_{ti}^1 \frac{\partial B_0}{\partial p_t^2} \right] \Big|_{p_t^2=m_t^2} \right. \\
&\quad \left. + (1 - 2A_{ti}^2) B_1 \right\} (p_t^2, m_{\bar{g}}^2, m_{\bar{t}_i}^2), \\
\delta Z_L^b &= -\frac{g_s^2 C_F}{16\pi^2} \left\{ m_b \left[ 2m_b \frac{\partial B_1}{\partial p_b^2} - m_{\bar{g}} A_{bi}^1 \frac{\partial B_0}{\partial p_b^2} \right] \Big|_{p_b^2=m_b^2} \right. \\
&\quad \left. + (1 - 2A_{bi}^2) B_1 \right\} (p_b^2, m_{\bar{g}}^2, m_{\bar{b}_i}^2), \\
\delta Z_R^t &= \delta Z_L^t (A_{ti}^2 \rightarrow -A_{ti}^2), \\
\delta Z_R^b &= \delta Z_L^b (A_{bi}^2 \rightarrow -A_{bi}^2), \\
\delta m_t/m_t &= \frac{g_s^2 C_F}{16\pi^2} (B_1 - \frac{m_{\bar{g}}}{m_t} A_{ti}^1 B_0) (p_t^2, m_{\bar{g}}^2, m_{\bar{t}_i}^2), \\
\delta m_b/m_b &= \frac{g_s^2 C_F}{16\pi^2} (B_1 - \frac{m_{\bar{g}}}{m_b} A_{bi}^1 B_0) (p_b^2, m_{\bar{g}}^2, m_{\bar{b}_i}^2), \quad (5.13)
\end{aligned}$$

where the color factor  $C_F = 4/3$ , and the renormalized self energy contributions from quarks as follows

$$\begin{aligned}
\hat{\Sigma}_S^t &= \frac{g_s^2 C_F}{16\pi^2} \frac{m_{\bar{g}}}{m_t} A_{ti}^1 \left[ B_0 (m_t^2, m_{\bar{g}}^2, m_{\bar{t}_i}^2) - B_0 (\hat{t}, m_{\bar{g}}^2, m_{\bar{t}_i}^2) \right], \\
\hat{\Sigma}_S^b &= \frac{g_s^2 C_F}{16\pi^2} \frac{m_{\bar{g}}}{m_b} A_{bi}^1 \left[ B_0 (m_b^2, m_{\bar{g}}^2, m_{\bar{b}_i}^2) - B_0 (\hat{s}, m_{\bar{g}}^2, m_{\bar{b}_i}^2) \right], \\
\hat{\Sigma}_L^t &= -\frac{g_s^2 C_F}{16\pi^2} (1 - 2A_{ti}^2) B_1 (\hat{t}, m_{\bar{g}}^2, m_{\bar{t}_i}^2) - \delta Z_L^t, \\
\hat{\Sigma}_L^b &= -\frac{g_s^2 C_F}{16\pi^2} (1 - 2A_{bi}^2) B_1 (\hat{s}, m_{\bar{g}}^2, m_{\bar{b}_i}^2) - \delta Z_L^b, \\
\hat{\Sigma}_R^t &= \hat{\Sigma}_L^t (A_{ti}^2 \rightarrow -A_{ti}^2), \\
\hat{\Sigma}_R^b &= \hat{\Sigma}_L^b (A_{bi}^2 \rightarrow -A_{bi}^2). \quad (5.14)
\end{aligned}$$

- 
- [1] For a review, see, e.g., H. E. Haber, G. L. Kane, Phys. Rept. **117**, 75 (1985).  
[2] C. S. Li and J. M. Yang, Phys. Lett. B **315**, 367 (1993);  
C. S. Li, B. Q. Hu and J. M. Yang, D **47**, 2865 (1993).  
J. M. Yang, C. S. Li and B. Q. Hu, D **47**, 2872 (1993);  
J. A. Coarasa, D. Garcia, J. Guasch, R. A. Jimenez, J. Sola, Eur. Phys. J. C **2**, 373 (1998).  
[3] F. Borzumati, J.-L. Kneur, N. Polonsky, Phys. Rev. D **60**, 115011 (1999); J. G., Li, C. S. Li, Phys. Rev. **D62**, 053008 (2000); S.-H. Zhu, hep-ph/0112109.  
[4] H. E. Haber, M. J. Herrero, H. E. Logan, S. Peñaranda, S. Rigolin and D. Temes, hep-ph/0102169.  
[5] H. E. Haber, M. J. Herrero, H. E. Logan, S. Penaranda, S. Rigolin and D. Temes, Phys. Rev. **D 63**, 055004 (2001).

- [6] M. J. Herrero, S. Peñaranda and D. Temes, FTUAM 00/20; IFT-UAM/CSIC 00/42.  
[7] T. Appelquist and J. Carazzone, Phys. Rev. **D11**, 2856 (1975); hep-ph/9912516.  
[8] H. L. Lai, et al. (CTEQ collaboration), hep-ph/9903282.  
[9] J. F. Gunion and H. E. Harber, Nucl. Phys. **B272**, 1 (1986).  
[10] A. Djouadi, J. Kalinowski and M. Spira, Comp. Phys. Commun. **108**, 56 (1998).  
[11] H. N. Brown, *et al.*, Mu g-2 Collaboration, Phys. Rev. Lett. **86**, 2227 (2001).  
[12] Particle Physics Group. Eur. Phys. J. C, **15**, 274 (2000).  
[13] M. Carena, D. Garcia, U. Nierste and C. E. Wagner, Nucl. Phys. B **577** (2000) 88; H. Eberl, K. Hidaka, S. Kraml, W. Majerotto and Y. Yamada, Phys. Rev. D **62** (2000) 055006.

